Journal of Fluorine Chemistry 131 (2010) 883–887

Contents lists available at ScienceDirect

Journal of Fluorine Chemistry

journal homepage: www.elsevier.com/locate/fluor

Short communication

Photoluminescence properties of new BF_2 complexes with pyrazolone ligands: Dependence on volume and electronic effect of substituents

Hui-hui Zhang [a], Xiong Hu [a], Wei Dou [a], Wei-sheng Liu [a,b,*]

[a] College of Chemistry and Chemical Engineering and State Key Laboratory of Applied Organic Chemistry, Lanzhou University, Lanzhou 730000, China
[b] State Key Laboratory of Coordination Chemistry, Nanjing University, Nanjing 210093, China

ARTICLE INFO

Article history:
Received 4 February 2010
Received in revised form 12 April 2010
Accepted 20 May 2010
Available online 1 June 2010

Keywords:
Photoluminescence properties
Donor–acceptor architecture
Pyzarolone
BF_2 complexes
Charge transfer
Crystal structure

ABSTRACT

Novel fluorine–boron complexes with donor–acceptor architecture in which pyrazoline-1,3-diones were chosen as electron donors have been synthesized and well characterized. Correlation of the luminescence properties of the complex **2c** and its crystal structures was discussed. Well-ordered molecular packing in the crystal results in strong charge transfer interactions characterized by long excited-state lifetime. These fluorine–boron complexes show photophysical properties highly dependent on the solvent polarity and aggregation states. The substituents on the pyrazoline were found to have a significant impact on the solid-state luminescent properties. As a result, some significant differences in charge transfer modes were observed in the solid state among these complexes.

© 2010 Elsevier B.V. All rights reserved.

1. Introduction

Recently, some multifunctional fluorophores with donor–acceptor (D–A) architecture have been reported for their ambipolar charge transport property and high luminescence efficiency [1–4]. In addition, compounds with D–A architecture always show particular and strong intermolecular and intramolecular interaction due to their planar structure and large polarity in the solid state. Many fluorine–boron complexes with D–A structure have been designed [1,4] because that trivalent boron is a well known electron-deficient acceptor and can receive part of the negative charge from an electron donor via certain delocalized π-bridges. There are three main types of fluorine–boron complexes, classified as N,N double-dentate, N,O double-dentate and O,O double-dentate compounds. For the former two kinds of fluorine–boron complexes, BODIPY (boradipyrromethene) [5–8] and 1,3,2-dioxaborine [9–12] are their corresponding representatives. Furthermore, boron-dipyrromethenes (BODIPY) have been studied widely because of their excellent fluorescent properties. However, there are not many reports available on the generation of difluoroboron complexes with O,O double-dentate ligands, although dioxaborine complexes have excellent photophysical properties. For instance, these materials exhibit interesting fluorescence emission, first- and second-order nonlinear optical properties [13–15], ion sensing ability [16–18], and can serve as emissive and/or electron-transport layers in OLEDs [19,20]. In order to expand their application potential, the relationship between structure and photochemistry properties needs to be further investigated. Some reports showed that annelation of electron donor to the dioxaborine ring, formed into D–A structure, resulted in enhanced absorption and fluorescence of the corresponding dyes and improving resistance to hydrolysis [21,22]. In the present work, pyrazoline-1,3-diones were chosen as electron donors which are new heterocyclic donors with unique photochemical properties [23–28] and then a new D–A structure (Fig. 1) was constructed. Herein, we examined the effects of the substituents of the pyrazoline ligands on the luminescent properties of the light-emitting materials.

2. Results and discussion

2.1. Crystal analysis

In the solid state, X-ray crystallographic data can generally provide detailed and conclusive structural information for a given molecule. The crystal of **2c** for X-ray diffraction was obtained through volatilization of benzene solvent at room temperature. The structural model refinement details carried out by the least-squares method are given in Table 1. As shown in Fig. 2, the unit

* Corresponding author at: College of Chemistry and Chemical Engineering and State Key Laboratory of Applied Organic Chemistry, Lanzhou University, Tianshui South Street NO. 222, Lanzhou 730000, China. Tel.: +86 931 8915151; fax: +86 931 8912582.
E-mail addresses: liuws@lzu.edu.cn, zhanghh06@163.com (W.-s. Liu).

0022-1139/$ – see front matter © 2010 Elsevier B.V. All rights reserved.
doi:10.1016/j.jfluchem.2010.05.006

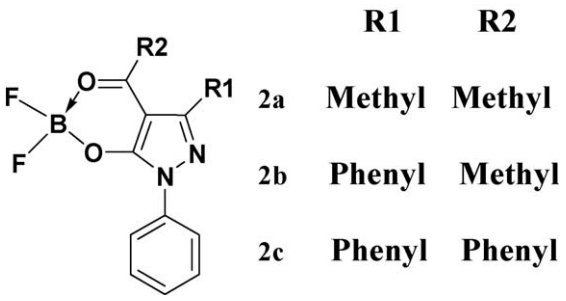

Fig. 1. Structures of **2a**, **2b** and **2c**.

cell contains two molecules in the crystal. Similar to the BF_2 complexes reported [29], the central six member ring containing O1–C7–C8–C16–O2 is almost coplanar with the adjacent pyrazolyl ring with the average deviation from the mean plane being 0.048 Å. The C7–C8 and C8–C16 bond lengths represent a bonding order of about 1.5, which indicates that the complexation of BF_2 increase the delocalization area of the π electrons in the β-diketone moiety. 1-Phenyl is almost coplanar with pyrazolyl ring with a twisting angle of 9.13° due to the existence of C–H...O and C–H...N hydrogen bonds. These phenomena indicate strong π-electron delocalization within the pyrazoline plane and the 1,3-diketone plane. The B–O bonds in the BF_2-chelating moiety are equivalent with their lengths for 1.495(4) Å and 1.493(3) Å, respectively. The BF_2 group in **2c** acts as a bifurcated acceptor with an angle of 113.0 (2)°, and one of F atoms forms C–H...F weak hydrogen bonds with the adjacent carbon of the phenyl ring with the distance of 3.180(4) Å and 3.237(4) Å (Fig. 3a). Due to dual C–H...F hydrogen-bonding interactions, the dioxaborine chelate ring is not planar. The relatively large deviation is observed between the plane of O1–B–O2 and the plane of O1–C7–C8–C16–O2 with a dihedral angle of 30.39°. Therefore, in sharp contrast to some reported BF_2 complexes [9,10,30,31], regular π–π stacking interactions between the layers cannot be observed in the solid state for **2c**. In the crystal, two molecules form a dimmer through a non-classical C–H...π hydrogen-bonding interaction which probably was induced by C–H...N hydrogen bond [32] (Fig. 3b). C20–H20...π aromatic centroid (C10, C11, C12, C13, C14, and C16) distance is 2.884 Å and the C20–H20...π centroid angle is 128.53°. The C–H...π interaction may result in the effective intermolecular charge transfer between two pyrazoline molecules. Adjacent molecules are linked by C–H...F and C–H...N hydrogen bonds which work as a major influencing factor on their π–π stacking, and thus two dimensional (2D) antiparallel columns are generated as shown in Fig. 3c. The well-ordered molecular packing is a favorable and critical factor in determining their electron-transporting properties for electron-optical materials based on small molecules.

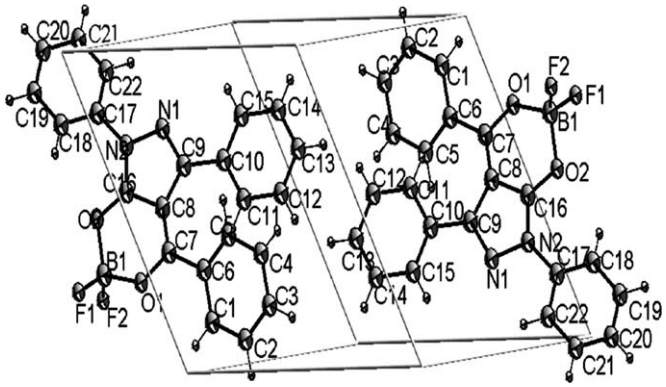

Fig. 2. Perspective view and labeling scheme for molecule **2c** in unit cell, thermal ellipsoids are at 30% probability level for C, O, N, B and F atoms. Selected bond lengths (Å): 1.300(3) (C7–O1), 1.379(3) (C7–C8), 1.394(3) (C8–C16), 1.300(3) (C16–O2);.

2.2. Electronic absorption and fluorescence spectra

Electronic absorption of the dioxaborine compounds in different solvents was measured in the region of 280–450 nm. As shown in Table 2, the maximum peaks show hypsochromic shifts with increase of the polarity of solvents, which indicates that these peaks originate from the π–π* transition. For **2c**, the absorption maximum is considerably red-shifted compared to those of **2a** and **2b**, due to the increased conjugation of dioxaborine and pyrazoline ring.

In toluene, compound **2a**, **2b** and **2c** exhibit fluorescence emission maximum at 355 nm when excited at 311 nm, which can be assigned to π–π* transition (Fig. 4). They show weak fluorescence intensities with 4.4%, 7.6% and 7.0% of absolute quantum yields for **2a**, **2b** and **2c**, respectively. Their broaden peaks in the longer wavelength region suggest mixing of the ICT character from N1–C1–N2–C3 in the pyrazoline. However, in $CHCl_3$, THF and acetonitrile, the emissions from **2a**, **2b** and **2c** cannot be observed, which may be due to strong ICT [33,34]. Unlike in solution, **2a**, **2b** and **2c** show fairly strong fluorescence intensity in the solid state, as displayed in Fig. 5. However, due to their strong absorption in the solid state, they exhibit lower absolute quantum yields than those in the toluene solution, with 3.0% for **2a**, 1.0% for **2b**, and 5.0% for **2c**. The emission maximum of **2c** red-shifts to 503 nm, and the emission bands of **2b** and **2a** are at 470 nm and 527 nm, respectively.

There are three features in their fluorescence spectra: a large Stokes shift, broad and fairly structureless emission spectra, and no mirror image relationship between the excitation and emission spectra. Their excitation bands get much broader and more intensive than in solution and red-shifted remarkably (Fig. 6). These features imply existence of charge transfer (CT) [35,36]. To

Table 1
Crystal data and structure refinement for complex **2c**.

Empirical formula	$C_{22}H_{15}BF_2N_2O_2$	*Dc* (g cm^{-3})	1.377
Formula weight	388.17	μ(Mo Kα) (mm^{-1})	0.100
Crystal system	Triclinic	F(0 0 0)	400
Space group	*P*-1	Data collected/unique	4699/3358
a (Å)	9.458 (7)	Limiting indices	$-10 \le h \le 11$
b (Å)	9.910 (7)		$-6 \le k \le 11$
c (Å)	11.165 (8)		$-13 \le l \le 13$
α (°)	87.085 (11)	*R1*, *wR2* ($I>2\sigma(I)$)	*R1* = 0.0433, *wR2* = 0.0967
β (°)	79.256 (10)	*R1*, *wR2* (all data)	*R1* = 0.0715, *wR2* = 0.1146
γ (°)	65.652 (10)	Parameter	262
V (Å3)	936.3 (11)	Goodness of fit on F^2	1.035
Crystal size (mm)	0.30 × 0.26 × 0.24	Δ(e Å^{-3}) (max, min)	0.15/−0.21
Z	2	–	–

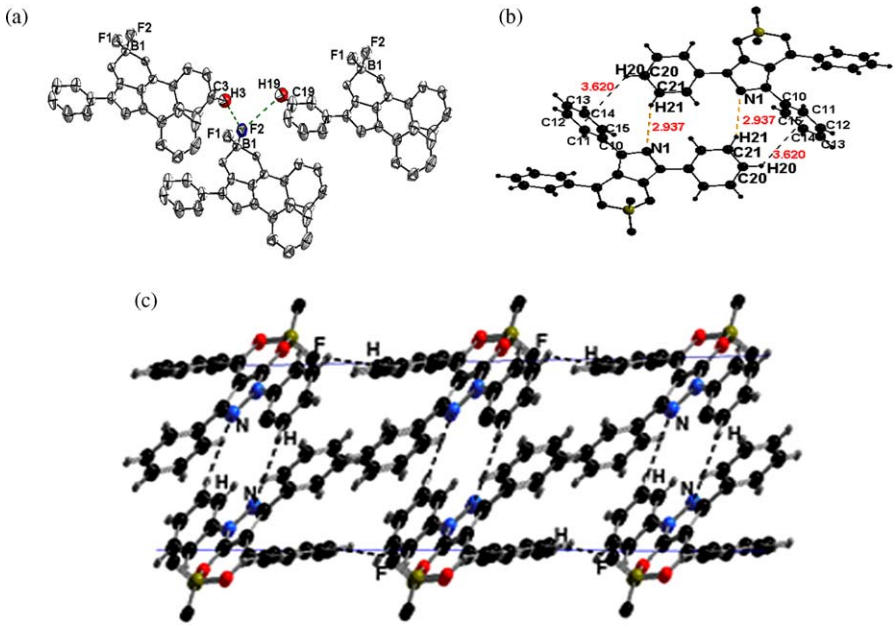

Fig. 3. (a) Views of hydrogen-bonding via C–H...F–B contacts in crystal **2c**; (b) views of C–H...π interaction between two pyrazoline molecules in crystal **2c**; (c) packing diagrams along the *a*-axis, showing the π–π contacts and network in crystal **2c**.

determine their emission origin in the solid state, absorption spectra in the solid state were measured (Fig. 7). A new fairly strong absorption bands for **2a**, **2b** and **2c**, due to aggregation of molecules, appear and are red-shifted compared to their corresponding absorption maxima in solution. The excitation spectra for **2a**, **2b** and **2c**, monitored at λ_{em} = 527 nm, 470 nm and 503 nm, respectively, are generally similar to their absorption spectra in the solid state. These observations indicate that the intermolecular charge transfer takes place in the ground state. Therefore, the excimer emission can be ruled out, which can be further confirmed by the evidence that there is no face-to-face π–π stacking structure in the solid state for **2c**. Excited-state lifetimes were measured for investigation of the emission transitions (Table 3). The luminescence decays of **2a** can be analyzed as sum of biexponentials that yields decay time 16.060 μs (60.66%), 116.390 μs (39.44%). The luminescence decays of **2c** can be analyzed as a sum of three exponentials that yield decay time 1.062 μs (12.66%), 10.466 μs (30.08%), 153.123 μs (57.26%). However, **2b** has the longest excited lifetime data in the millisecond range compared with **2a** and **2c**. The long lifetimes suggest that the emissions originate from intermolecular charge transfer state which is a stable and long-lived charge-separated state due to strong CT interactions inhibiting efficiently the back electron transfer [37]. From the lifetime data, there probably exist multiple emission decay modes corresponding to multiple CT interaction types [36]. Analyzing on solid structure of **2c**, there are two kinds of molecular aggregation: pyrazoline–pyrazoline (Py–Py) due to C–H...π and C–H...N hydrogen-bonding interaction and D–A...D–A pairs due to C–H...F hydrogen-bonding interaction, which causes emissions to red-shift and be broaden to some

Table 2
Maximum absorption peaks of the dyes **2a**, **2b** and **2c** in four representative solvents ($c = 2 \times 10^{-6}$ mol dm^{-3}).

	Toluene	THF	$CHCl_3$	Acetonitrile
2a	288	284	283	281
2b	292	283	284	278
2c	327	323	322	315

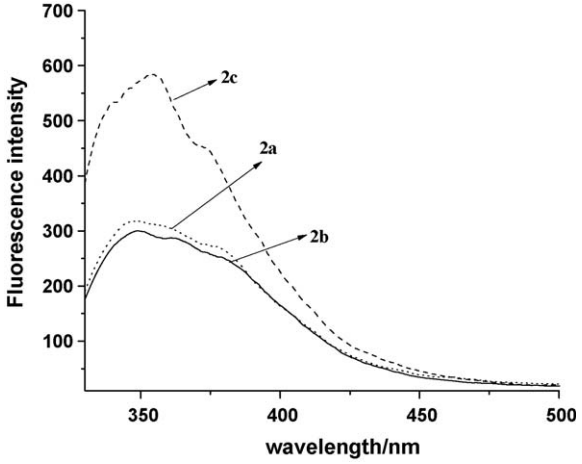

Fig. 4. Fluorescence spectra of **2a**, **2b** and **2c** in toluene solvent, λ_{exi} = 311 nm.

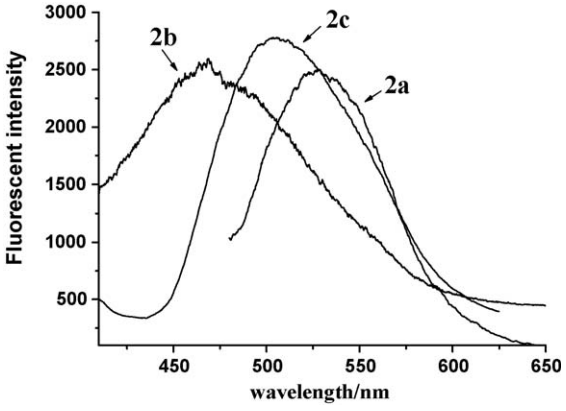

Fig. 5. Fluorescence spectra of **2a**, **2b** and **2c** in the solid state, λ_{exi} (**2a**) = 470 nm, λ_{exi} (**2b**) = 373 nm, and λ_{exi} (**2c**) = 420 nm.

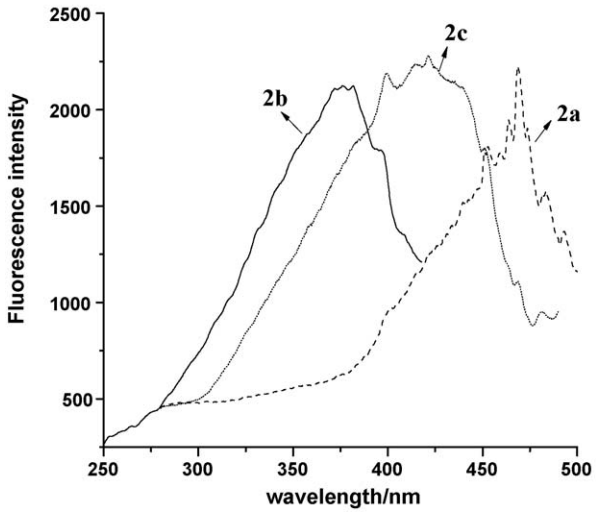

Fig. 6. Excitation spectra of **2a**, **2b** and **2c** in the solid state, λ_{emi} (**2a**) = 527 nm, λ_{emi} (**2b**) = 470 nm, and λ_{emi} (**2c**) = 503 nm.

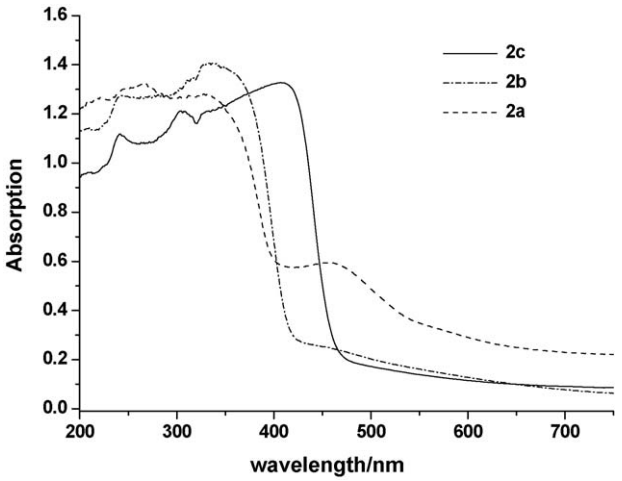

Fig. 7. Absorption spectra of **2a**, **2b** and **2c** in the solid state.

Table 3
The fluorescence decay times of different samples in the solid state at room temperature.

Sample	Excitation wavelength/nm	Monitored wavelength/nm	$\tau/\mu s$[a]		
2a	470	527	16.060 (60.66%)	116.390 (39.44%)	
2b	373	470	2085.075		
2c	420	503	1.062 (12.66%)	10.466 (30.08%)	153.123 (57.26%)

[a] The data in the bracket show the percentage of excited-state lifetime.

extent (Fig. 3b). However, the volume and the electronic effect of substituent groups should be considered factors on the molecular aggregation effects when molecules are approaching among them. So, **2a**, **2b** and **2c** exhibit different emission spectra remarkably with the changes of the substituent groups at 3,4-positions. This suggests that the spatial configuration of these molecules in the solid state plays an important role in their photoluminescence properties.

3. Conclusions

In conclusion, the fluorine–boron complexes with donor–acceptor architecture exhibit significant differences in luminescent behaviors with the changes of the electronic effect of substituents at the 3,4-position on the pyrazoline. Well-ordered molecular packing in the crystals results in strong charge transfer interactions characterized by long excited-state lifetime.

4. Experimental

4.1. Materials and methods

All chemicals were obtained from commercial suppliers and used without further purification. $CHCl_3$ and CH_3CN were dried over CaH_2 overnight under nitrogen before distillation. Electronic absorption spectra in chloroform solution were obtained by using Varian UV-Cary 100 spectrophotometer. Electronic absorption spectra in the solid state were measured in Varian UV-Cary 5000 spectrophotometer with diffuse reflectance method by using 110 mm integrating sphere accessory. ^1H NMR and ^{13}C NMR spectra were measured on a Varian Mercury plus 400 MHz spectrometer in $CDCl_3$ solution with TMS as internal standard. Fluorescence measurements were made on a Hitachi F-4500 spectrophotometer equipped with quartz cuvettes of 1 cm path length at room temperature. Quantum yields were determined by an absolute method using an integrating sphere on FLS 920 of Edinburgh Instrument. Fluorescence lifetimes were recorded on a single-photon-counting spectrophotometer from Edinburgh Instruments (FLS 920) with nanosecond pulse lamp as the excitation source. The emission of a sample was collected by two lenses into a monochromator (WDG30), detected by a photomultiplier and processed by a Boxcar Average (EGG model 162) in line with a microcomputer. Single-crystal X-ray diffraction measurements were carried out on a Bruker SMART 1000 CCD diffractometer operating at 50 kV and 30 mA using Mo Kα radiation (λ = 0.71073 Å). Each selected crystal was mounted inside a Lindemann glass capillary for data collection using the SMART and SAINT software. An empirical absorption correction was applied using the SADABS program. All the structures were solved by direct methods and refined by full-matrix least-squares on F^2 using the SHELXTL-97 program package [38].

4.2. Synthesis of boron complexes

The 4-acyl-5-hydroxyl-3-methyl-phenylpyrazolone, 4-acyl-5-hydroxyl-1,3-diph enylpyrazolone and 4-benzoyl-5-hydroxyl-1,3-diphenylpyrazolones (**1a**, **1b**, and **1c**) were synthesized by the procedure reported by Jensen [39]. The dioxaborine complexes (**2a**, **2b** and **2c**) were prepared by pyrazolone and 10 equivalents of BF_3/ether adduct in little amount of CH_2Cl_2 solvent.

4.2.1. (O_1-B)-1-[4′-[(Difluoroboryl)oxy]-(5-hydroxy-3-methyl-1-phenyl-1H-pyrazol-4-yl)] ethan-1-one (2a)

Boron trifluoride–diethyl etherate (3.8 mL, 29.4 mmol) was added to a solution of 4-acyl-5-hydroxyl-3-methyl-phenylpyrazolones (0.65 g, 3 mmol) in dry dichloro- methane (10 mL) under nitrogen. The reaction mixture was stirred for 3 h. After removal of the solvent, the residue was filtered and washed with hexane. The

solid was purified by recrystallization in benzene solvent to provide boron complex **2a** as light yellow needles with a yield of 0.47 g (60% yield). M.p. 224.0–224.6 °C. IR (KBr): 1616, 1565, 1502, 1066, 1028 cm^{-1}. ^1H NMR (400 MHz, $CDCl_3$) δ(ppm): 7.86 (dd, 2H, J = 8 Hz, 1-ArH), 7.48 (t, 2H, J = 8 Hz, 1-ArH), 7.36 (t, 1H, J = 7.4 Hz, 1-ArH), 2.65 (s, 3H, 4-CH_3), 2.53 (s, 3H, 3-CH_3). Anal. Calcd for $C_{12}H_{11}BF_2N_2O_2$: C, 54.59; H, 4.20; N, 10.61; found: C, 54.30; H, 4.12; N, 10.52.

Similar reaction conditions were applied to the synthesis of boron complexes **2b** and **2c**.

*4.2.2. (O_1-B)-1-[4′-[(Difluoroboryl)oxy]-(5-hydroxy-1,3-diphenyl-1H-pyrazol-4-yl)]ethan-1-one (**2b**)*

Colorless powder: yield 75%. M.p. 192.4–192.7°C. IR (KBr): 1615, 1565, 1502, 1071, 1034 cm^{-1}. ^1H NMR (400 MHz, $CDCl_3$) δ(ppm): 7.95 (d, 2H, J = 8 Hz, 1-ArH), 7.62 (d, 2H, J = 7.2 Hz, 1-ArH), 7.52 (m, 5H, 3-ArH), 7.39 (t, 1H, J = 7.2 Hz, 1-ArH), 2.44 (s, 3H, 4-CH_3). Anal. Calcd for $C_{17}H_{13}BF_2N_2O_2$: C, 62.61; H, 4.02; N, 8.59; found: C, 62.54; H, 3.95; N, 8.49.

*4.2.3. (O_1-B)-1-[4′-[(Difluoroboryl)oxy]-(5-hydroxy-1,3-diphenyl-1H-pyrazol-4-yl) (phenyl)]methanone (**2c**)*

Yellow block crystal: yield 80%. M.p. 186.6–187.5°C IR (KBr):1603, 1525, 1493, 1070, 1034 cm^{-1}. ^1H NMR (400 MHz, $CDCl_3$) δ(ppm): 8.02 (d, 2H, J = 8 Hz, 1-ArH), 7.59 (d, 2H, J = 8 Hz, 1-ArH), 7.53 (q, 3H, J = 8 Hz, 4-ArH), 7.43 (d, 1H, J = 7.2 Hz, 1-ArH), 7.33 (m, 3H, 3-ArH), 7.24 (m, 2H, 4-ArH), 7.21 (m, 2H, 3-ArH). Anal. Calcd for $C_{22}H_{15}BF_2N_2O_2$: C, 68.07; H, 3.89; N, 7.22; found: C, 68.01; H, 3.78; N, 7.18. The crystal of **2c** for X-ray diffraction was obtained through volatilization of benzene solvent at room temperature.

Supplementary material

Crystallographic data for **2c** have been deposited at the Cambridge Crystallographic Data Center with the deposition number of CCDC 720403. These data can be obtained free of charge from the Cambridge Crystallographic Data Center via www.ccdc.cam.ac.uk/conts/retrieving.html [or from the Cambridge Crystallographic Data Center, 12 Union Road, Cambridge CB2 1EZ, UK; E-mail:deposit@ccdc.cam.ac.uk].

Acknowledgement

The work was supported by the NSFC (Grants 20771048 and 20621091).

References

[1] W. Jia, X. Feng, D. Bai, Z. Lu, S. Wang, G. Vamvounis, Chem. Mater. 17 (2005) 164–170.
[2] K.R.J. Thomas, J.T. Lin, M. Velusamy, Y. Tao, C. Chuen, Adv. Funct. Mater. 14 (2004) 83–90.
[3] Y. Shirota, M. Kinoshita, T. Noda, K. Okumoto, T. Ohara, J. Am. Chem. Soc. 122 (2000) 11021–11022.
[4] Z.Q. Liu, Q. Fang, D. Wang, G. Xue, W.T. Yu, Z.S. Shao, M.H. Jiang, Chem. Commun. (2002) 2900–2901.
[5] P. Oleynik, Y. Ishihara, G. Cosa, J. Am. Chem. Soc. 129 (2007) 1842–1843.
[6] T. Yogo, Y. Urano, Y. Ishitsuka, F. Maniwa, T. Nagano, J. Am. Chem. Soc. 127 (2005) 12162–12163.
[7] Z. Li, E. Mintzer, R. Bittman, J. Org. Chem. 71 (2006) 1718–1721.
[8] M. Baruah, W. Qin, N. Basaric, W.M. DeBorggraeve, N. Boens, J. Org. Chem. 70 (2005) 4152–4157.
[9] D. Rohde, C.J. Yan, L.J. Wan, Langmuir 22 (2006) 4750–4757.
[10] B. Domercq, C. Grasso, J.L. Maldonado, M. Halik, S. Barlow, S.R. Marder, B. Kippelen, J. Phys. Chem. B 108 (2004) 8647–8651.
[11] C. Risko, E. Zojer, P. Brocorens, S.R. Marder, J.L. Bredas, Chem. Phys. 313 (2005) 151–157.
[12] V.F. Traven, A.V. Manaev, T.A. Chibisova, J. Electron Spectrosc. Relat. Phenom. 149 (2005) 6–10.
[13] J.M. Hales, S. Zheng, S. Barlow, S.R. Marder, J.W. Perry, J. Am. Chem. Soc. 128 (2006) 11362–11363.
[14] R. Kammler, G. Bourhill, Y. Jin, C. Brauchle, G. Gorlitz, H. Hartmann, J. Chem. Soc., Faraday Trans. 92 (1996) 945–947.
[15] E. Cogné-Laage, J.F. Allemand, O. Ruel, J.B. Baudin, V. Croquette, M. Blanchard-Desce, L. Jullien, Chem. Eur. J. 10 (2004) 1445–1455.
[16] Z.Q. Liu, M. Shi, F.Y. Li, Q. Fang, Z.H. Chen, T. Yi, C.H. Huang, Org. Lett. 7 (2005) 5481–5484.
[17] C. Fujimoto, Y. Kusunose, H. Maeda, J. Org. Chem. 71 (2006) 2389–2394.
[18] H. Maeda, Y. Haketa, Y. Bando, S. Sakamoto, Synth. Met. 159 (2009) 792–796.
[19] C.D. Entwistle, T.B. Marder, Chem. Mater. 16 (2004) 4574–4585.
[20] Y.Q. Li, Y. Liu, W.M. Bu, J.H. Guo, Y. Wang, Chem. Commun. (2000) 1551–1552.
[21] A.O. Gerasov, M.P. Shandura, Y.P. Kovtun, Dyes Pigments 79 (2008) 252–258.
[22] V.F. Traven, T.A. Chibisova, A.V. Manaev, Dyes Pigments 58 (2003) 41–46.
[23] Z.L. Yan, G.W. Hu, S.K. Wu, Acta Chim. Sin. 53 (1995) 227–233.
[24] A. Wagner, C.W. Schellhammer, S. Petersen, Angew. Chem. Int. Ed. 5 (1966) 699–704.
[25] H. Dorlars, C.W. Schellhammer, J. Schroeder, Angew. Chem. Int. Ed. 14 (1975) 665–679.
[26] A.K. Sarkar, Fluorescent Whitening Agents, Merrow, Watford, England, 1971.
[27] S.J. Ji, H.B. Shi, Dyes Pigments 70 (2006) 246–250.
[28] T. Sano, T. Fujii, Y. Nishio, Y. Hamada, K. Shibata, K. Kuroki, Jpn. J. Appl. Phys. 34 (1995) 3124–3127.
[29] J. Christoffers, B. Kreidler, S. Unger, W. Frey, Eur. J. Org. Chem. (2003) 2845–2853.
[30] A.G. Mirochnik, B.V. Bukvetskii, E.V. Gukhman, V.E. Karasev, J. Fluoresc. 13 (2003) 157–162.
[31] D. Plazuk, A. Klys, J. Zakrzewski, A. Rybarczyk-Pirek, T.A. Olszak, Organometallics 20 (2001) 4448–4450.
[32] D. Escudero, A. Frontera, D. Quiñonero, P.M. Deyà, J. Phys. Chem. A 112 (2008) 6017–6022.
[33] Z.R. Grabowski, K. Rotkiewicz, W. Rettig, Chem. Rev. 103 (2003) 3899–4032.
[34] E.M. Kosower, Acc. Chem. Res. 15 (1982) 259–266.
[35] T. Akutagawa, T. Nakamura, Cryst. Growth Des. 6 (2006) 70–74.
[36] H.B. Fu, B.H. Loo, D.B. Xiao, R.M. Xie, X.H. Ji, J.N. Yao, B.W. Zhang, L.Q. Zhang, Angew. Chem. Int. Ed. 41 (2002) 962–965.
[37] G.H. Zhang, J.K. Thomas, J. Phys. Chem. B 107 (2003) 7254–7260.
[38] G.M. Sheldrick, SHELXL-97, Program for the Solution of Crystal Structures, University of Göttingen, Göttingen, Germany, 1997.
[39] B.S. Jensen, Acta Chem. Scand. 13 (1959) 1347–1357.